The Astronomical Journal, 127:3023–3033, 2004 May

EXTREME KUIPER BELT OBJECT 2001 QG_{298} AND THE FRACTION OF CONTACT BINARIES

Scott S. Sheppard and David C. Jewitt[1]
Institute for Astronomy, University of Hawaii, 2680 Woodlawn Drive, Honolulu, HI 96822;
sheppard@ifa.hawaii.edu, jewitt@ifa.hawaii.edu
Received 2003 December 23; accepted 2004 February 11

ABSTRACT

Extensive time-resolved observations of Kuiper belt object 2001 QG_{298} show a light curve with a peak-to-peak variation of 1.14 ± 0.04 mag and single-peaked period of 6.8872 ± 0.0002 hr. The mean absolute magnitude is 6.85 mag, which corresponds to a mean effective radius of 122 (77) km if an albedo of 0.04 (0.10) is assumed. This is the first known Kuiper belt object and only the third minor planet with a radius greater than 25 km to display a light curve with a range in excess of 1 mag. We find the colors to be typical for a Kuiper belt object ($B-V = 1.00 \pm 0.04$, $V-R = 0.60 \pm 0.02$), with no variation in color between minimum and maximum light. The large light variation, relatively long double-peaked period, and absence of rotational color change argue against explanations due to albedo markings or elongation due to high angular momentum. Instead, we suggest that 2001 QG_{298} may be a very close or contact binary, similar in structure to what has been independently proposed for the Trojan asteroid 624 Hektor. If so, its rotational period would be twice the light-curve period, or 13.7744 ± 0.0004 hr. By correcting for the effects of projection, we estimate that the fraction of similar objects in the Kuiper belt is at least ~10% to 20%, with the true fraction probably much higher. A high abundance of close and contact binaries is expected in some scenarios for the evolution of binary Kuiper belt objects.

Key words: Kuiper belt — minor planets, asteroids — solar system: general

1. INTRODUCTION

The Kuiper belt is a long-lived region of the solar system just beyond Neptune where the planetesimals have not coalesced into a planet. It contains about 80,000 objects with radii greater than 50 km (Trujillo, Jewitt, & Luu 2001) that have been collisionally processed and gravitationally perturbed throughout the age of the solar system. The short-period comets and Centaurs are believed to originate from the Kuiper belt (Fernández 1980; Duncan, Quinn, & Tremaine 1988).

Physically, the Kuiper belt objects (KBOs) show a large diversity of colors, from slightly blue to ultrared ($V-R \sim 0.3$ to $V-R \sim 0.8$; Luu & Jewitt 1996), and may show correlations between colors, inclination, and perihelion distance (Jewitt & Luu 2001; Trujillo & Brown 2002; Doressoundiram et al. 2002; Tegler & Romanishin 2003). Spectra of KBOs are mostly featureless, with a few showing hints of water ice (Brown, Cruikshank, & Pendleton 1999; Jewitt & Luu 2001; Lazzarin et al. 2003). The range of KBO geometric albedos is still poorly sampled, but the larger ones likely have values between 0.04 and 0.10 (Jewitt, Aussel, & Evans 2001; Altenhoff, Bertoldi, & Menten 2004). Time-resolved observations of KBOs show that ~32% vary by $\geq$0.15 mag, 18% by $\geq$0.40 mag, and 12% by $\geq$0.60 mag (Sheppard & Jewitt 2002; Ortiz et al. 2003; Lacerda & Luu 2003; Sheppard & Jewitt 2004). One object, (20000) Varuna, displays a large photometric range and fast rotation and is best interpreted as a structurally weak object elongated by its own rotational angular momentum (Jewitt & Sheppard 2002). A significant fraction of KBOs appear to be more elongated than main-belt asteroids of similar size (Sheppard & Jewitt 2002). The KBO phase functions are steep, with a median of 0.16 mag deg^{-1} between phase angles of 0° and 2° (Sheppard & Jewitt 2002; Schaefer & Rabinowitz 2002; Sheppard & Jewitt 2004).

About 4% ± 2% of the KBOs are binaries with separations $\geq$0\.15 (Noll et al. 2002), while binaries with separations $\geq$0\.1 may constitute about 15% of the population (C. Trujillo 2003, private communication). All the binary KBOs found to date appear to have mass ratios near unity, though this may be an observational selection effect. The mechanism responsible for creating KBO binaries is not clear. Formation through collisions is unlikely (Stern 2002). Weidenschilling (2002) has proposed formation of such binaries through complex three-body interactions, which would only occur efficiently in a much higher population of large KBOs than can currently be accounted for. Goldreich, Lithwick, & Sari (2002) have proposed that KBO binaries could be formed when two bodies approach each other and energy is extracted either by dynamical friction from the surrounding sea of smaller KBOs or by a close third body. This process also requires that the density of KBOs was ~10^2 to 10^3 times greater than now. They predict that closer binaries should be more abundant in the Kuiper belt, while Weidenschilling's mechanism predicts the opposite.

The present paper is the fourth in a series resulting from the Hawaii Kuiper Belt Variability Project (HKBVP; see Jewitt & Sheppard 2002; Sheppard & Jewitt 2002, 2004). The practical aim of the project is to determine the rotational characteristics (principally, period and shape) of bright KBOs ($m_R \leq 22$) in order to learn about the distributions of rotation period and shape in these objects. In the course of this survey we found that 2001 QG_{298} has an extremely large light variation and a relatively long period. We have obtained optical observations of 2001 QG_{298} in order to accurately determine the rotational light curve and constrain its possible causes. This object has a typical Plutino orbit in 3 : 2 mean motion resonance with

[1] Visiting Astronomer, W. M. Keck Observatory, which is operated as a scientific partnership among the California Institute of Technology, the University of California, and the National Aeronautics and Space Administration. The Observatory was made possible by the generous financial support of the W. M. Keck Foundation.

Neptune, semimajor axis at 39.2 AU, eccentricity of 0.19, and inclination of 6°.5.

2. OBSERVATIONS

We used the University of Hawaii (UH) 2.2 m diameter telescope atop Mauna Kea in Hawaii to obtain *R*-band observations of 2001 QG_{298} on three separate observing runs each covering several nights: UT 2002 September 12 and 13; 2003 August 22, 26, 27, and 28; and 2003 September 27, 28, and 30. Two different CCD cameras were employed. For the 2002 September and 2003 September observations, we used a 2048 × 2048 pixel Tektronix CCD (24 μm pixels) camera with a 0″.219 pixel^{-1} scale at the f/10 Cassegrain focus. An antireflection coating on the CCD gave very high average quantum efficiency (0.90) in the *R* band. The field of view was 7′.5 × 7′.5. For the 2003 August observations, we used the Orthogonal Parallel Transfer Imaging Camera (OPTIC). OPTIC has two 4104 × 2048 pixel Lincoln Laboratory CCID28 orthogonal transfer CCDs, developed to compensate for real-time image motion by moving the charge on the chips to compensate for seeing variations (Tonry, Burke, & Schechter 1997). Howell et al. (2003) have demonstrated that these chips are photometrically accurate and provide routine sharpening of the image point-spread function. There is a ∼15″ gap between the chips. The total field of view was 9′.5 × 9′.5 with 15 μm pixels, which corresponds to 0″.14 pixel^{-1} scale at the f/10 Cassegrain focus. The same *R*-band filter based on the Johnson-Kron-Cousins photometric system was used for all UH 2.2 m observations.

In addition, we used the 10 m Keck I Telescope to obtain *BVR* colors of 2001 QG_{298} at its maximum and minimum light on UT 2003 August 30. The LRIS camera with its Tektronix 2048 × 2048 pixel CCD and 24 μm pixels (image scale 0″.215 pixel^{-1}) was used (Oke et al. 1995) with the facility broadband *BVR* filter set. Because of a technical problem with the blue camera side, we used only the red side for photometry at *B*, *V*, and *R*. The blue filter response was cut by the use of a dichroic at 0.460 μm.

All exposures were taken in a consistent manner with the telescope autoguided on bright nearby stars. The seeing ranged from 0″.6 to 1″.0 during the various observations; 2001 QG_{298} moved relative to the fixed stars at a maximum of 3″.5 hr^{-1}, corresponding to trail lengths ≤0″.43 in the longest (450 s) exposures. Thus, motion of the object was insignificant compared with the seeing.

Images from the UH telescope were bias-subtracted and then flat-fielded using the median of a set of dithered images of the twilight sky. Data from Keck were bias-subtracted and flattened using flat fields obtained from an illuminated spot inside the closed dome. Landolt (1992) standard stars were employed for the absolute photometric calibration. To optimize the signal-to-noise ratio, we performed aperture correction photometry by using a small aperture on 2001 QG_{298} (0″.65 to 0″.88 in radius) and both the same small aperture and a large aperture (2″.40 to 3″.29 in radius) on (four or more) nearby bright field stars. We corrected the magnitude within the small aperture used for the KBOs by determining the correction from the small to the large aperture using the field stars (cf. Tegler & Romanishin 2000; Jewitt & Luu 2001; Sheppard & Jewitt 2002). Since 2001 QG_{298} moved slowly, we were able to use the same field stars from night to night within each observing run, resulting in very stable relative photometric calibration from night to night. The observational geometry for 2001 QG_{298} on each night of observation is shown in Table 1.

3. RESULTS

Tables 2 and 3 show the photometric results for 2001 QG_{298}. We used the phase dispersion minimization (PDM) method (Stellingwerf 1978) to search for periodicity in the data. In PDM, the metric is the so-called Θ-parameter, which is essentially the variance of the unphased data divided by the variance of the data when phased by a given period. The best-fit period should have a very small dispersion compared with the unphased data, and thus $\Theta \ll 1$ indicates that a good fit has been found.

Substantial variability was shown by 2001 QG_{298} (∼1.1 mag, with a single-peaked period near 6.9 hr) in *R*-band observations from two nights in 2002 September. We obtained further observations of the object in 2003 to determine the light curve with greater accuracy. PDM analysis of all the apparent magnitude *R*-band data from the 2002 September and 2003 August and September observations show that 2001 QG_{298} has strong Θ minima near the periods $P = 6.88$ hr and $P = 13.77$ hr, with weaker alias periods flanking these (Fig. 1). We corrected the apparent magnitude data for the minor phase-angle effects (we used the nominal 0.16 mag deg^{-1} found in Sheppard & Jewitt 2002, 2004) and light-travel time differences of the observations to correspond to the 2003 August 30 observations. We then phased the data to all the peaks with $\Theta < 0.4$ and found only the 6.8872 and 13.7744 hr periods to be consistent with all the data (Figs. 2 and 3). Through a closer look at the PDM plot (Fig. 4) and phasing the data, we find best-fit periods $P = 6.8872 \pm 0.0002$ hr (a light curve with a single maximum per period) and $P = 13.7744 \pm 0.0004$ hr (two maxima per period, as expected for rotational modulation caused by an aspherical shape). The double-peaked light curve appears to be the best fit, with the minima different by about 0.1 mag, while the maxima appear to be of similar brightness. The photometric range of the light curve is $\Delta m = 1.14 \pm 0.04$ mag.

The Keck *BVR* colors of 2001 QG_{298} show no variation from minimum to maximum light within the photometric uncertainties of a few percent (see Figs. 2 and 3). This is again consistent with a light curve that is produced by an elongated shape, rather than by albedo variations. The colors ($B-V = 1.00 \pm 0.04$, $V-R = 0.60 \pm 0.02$) show that 2001 QG_{298} is red and similar to the mean values ($B-V = 0.98 \pm 0.04$, $V-R = 0.61 \pm 0.02$; 28 objects) for KBOs as a group (Jewitt & Luu 2001).

TABLE 1
GEOMETRIC CIRCUMSTANCES OF THE OBSERVATIONS

UT Date	R (AU)	Δ (AU)	α (deg)
2002 Sep 12	32.0028	30.9994	0.151
2002 Sep 13	32.0026	30.9983	0.119
2003 Aug 22	31.9392	31.0405	0.851
2003 Aug 26	31.9385	31.0112	0.738
2003 Aug 27	31.9384	31.0046	0.709
2003 Aug 28	31.9382	30.9982	0.680
2003 Aug 30	31.9378	30.9863	0.622
2003 Sep 27	31.9330	30.9407	0.253
2003 Sep 28	31.9328	30.9434	0.283
2003 Sep 30	31.9325	30.9497	0.345

TABLE 2

R-Band Observations at the UH 2.2 Meter Telescope

Image[a]	UT Date[b]	Julian Date[c]	Exp.[d] (s)	m_R[e] (mag)
nt3023	2002 Sep 12.32535	2,452,529.825347	450	21.673
nt3024	2002 Sep 12.33185	2,452,529.831840	450	21.542
nt3025	2002 Sep 12.33836	2,452,529.838356	450	21.539
nt3028	2002 Sep 12.35733	2,452,529.857326	450	21.429
nt3029	2002 Sep 12.36383	2,452,529.863819	450	21.396
nt3030	2002 Sep 12.37045	2,452,529.870451	400	21.311
nt3031	2002 Sep 12.37646	2,452,529.876458	400	21.351
nt3034	2002 Sep 12.39474	2,452,529.894734	400	21.282
nt3035	2002 Sep 12.40065	2,452,529.900648	400	21.281
nt3038	2002 Sep 12.42219	2,452,529.922188	400	21.315
nt3039	2002 Sep 12.42811	2,452,529.928102	400	21.299
nt3043	2002 Sep 12.45360	2,452,529.953600	400	21.440
nt3044	2002 Sep 12.45952	2,452,529.959514	400	21.560
nt4047	2002 Sep 13.32242	2,452,530.822419	350	21.398
nt4048	2002 Sep 13.32776	2,452,530.827755	350	21.476
nt4071	2002 Sep 13.40951	2,452,530.909514	400	22.458
nt4072	2002 Sep 13.41544	2,452,530.915428	400	22.377
nt4083	2002 Sep 13.44672	2,452,530.946725	400	22.004
nt4084	2002 Sep 13.45264	2,452,530.952639	400	21.906
nt4097	2002 Sep 13.50026	2,452,531.000255	400	21.427
nt4098	2002 Sep 13.50617	2,452,531.006169	400	21.438
nt4112	2002 Sep 13.56040	2,452,531.060394	400	21.249
nt4113	2002 Sep 13.56631	2,452,531.066308	400	21.259
f.114	2003 Aug 22.44983	2,452,873.949815	400	21.356
f.115	2003 Aug 22.46309	2,452,873.963079	400	21.341
f.116	2003 Aug 22.46815	2,452,873.968125	400	21.315
f.117	2003 Aug 22.47331	2,452,873.973287	380	21.381
f.118	2003 Aug 22.47812	2,452,873.978090	380	21.343
f.119	2003 Aug 22.48288	2,452,873.982859	380	21.312
f.124	2003 Aug 22.51473	2,452,874.014711	380	21.375
f.125	2003 Aug 22.51984	2,452,874.019815	380	21.452
f.126	2003 Aug 22.52467	2,452,874.024630	380	21.425
f.127	2003 Aug 22.53082	2,452,874.030799	380	21.521
f.128	2003 Aug 22.53559	2,452,874.035567	380	21.549
f.138	2003 Aug 22.57113	2,452,874.071111	380	21.808
f.139	2003 Aug 22.57589	2,452,874.075868	380	21.899
f.140	2003 Aug 22.58063	2,452,874.080613	380	21.946
f.141	2003 Aug 22.58543	2,452,874.085405	380	21.993
f.142	2003 Aug 22.59016	2,452,874.090150	380	22.069
f.143	2003 Aug 22.59494	2,452,874.094919	380	22.093
f.144	2003 Aug 22.59972	2,452,874.099699	380	22.150
f.147	2003 Aug 22.61900	2,452,874.118981	380	22.460
f.148	2003 Aug 22.62375	2,452,874.123738	380	22.444
nt1115	2003 Aug 26.52466	2,452,878.024653	300	21.383
nt1116	2003 Aug 26.52830	2,452,878.028287	300	21.390
nt1137	2003 Aug 26.56556	2,452,878.065544	400	21.565
nt1138	2003 Aug 26.57085	2,452,878.070833	400	21.667
nt1141	2003 Aug 26.58721	2,452,878.087187	400	21.843
nt1142	2003 Aug 26.59203	2,452,878.092014	400	21.784
nt1145	2003 Aug 26.60817	2,452,878.108171	400	22.045
nt1146	2003 Aug 26.61414	2,452,878.114120	400	22.150
nt2057	2003 Aug 27.34245	2,452,878.842442	400	21.289
nt2058	2003 Aug 27.34729	2,452,878.847280	400	21.336
nt2068	2003 Aug 27.37572	2,452,878.875706	400	21.377
nt2069	2003 Aug 27.38053	2,452,878.880521	400	21.380
nt2072	2003 Aug 27.40915	2,452,878.909144	400	21.443
nt2073	2003 Aug 27.41403	2,452,878.914016	400	21.509
nt2080	2003 Aug 27.43887	2,452,878.938854	400	21.717
nt2081	2003 Aug 27.44368	2,452,878.943669	400	21.792
nt2090	2003 Aug 27.46950	2,452,878.969479	400	22.072
nt2091	2003 Aug 27.47431	2,452,878.974294	400	22.094
nt2098	2003 Aug 27.49900	2,452,878.998981	400	22.315
nt2099	2003 Aug 27.50382	2,452,879.003808	400	22.382
nt2104	2003 Aug 27.52311	2,452,879.023090	400	22.168

TABLE 2—*Continued*

Image[a]	UT Date[b]	Julian Date[c]	Exp.[d] (s)	m_R[e] (mag)
nt2105	2003 Aug 27.52795	2,452,879.027928	400	22.070
nt2108	2003 Aug 27.54033	2,452,879.040324	400	21.884
nt2109	2003 Aug 27.54516	2,452,879.045139	400	21.826
nt2114	2003 Aug 27.56485	2,452,879.064826	400	21.648
nt2115	2003 Aug 27.56971	2,452,879.069688	400	21.614
nt2122	2003 Aug 27.59367	2,452,879.093657	400	21.461
nt2123	2003 Aug 27.59849	2,452,879.098472	400	21.460
nt2127	2003 Aug 27.61524	2,452,879.115220	400	21.367
nt2128	2003 Aug 27.62006	2,452,879.120046	400	21.378
nt3062	2003 Aug 28.29908	2,452,879.799074	400	21.752
nt3063	2003 Aug 28.30389	2,452,879.803877	400	21.805
nt3066	2003 Aug 28.32106	2,452,879.821053	400	22.002
nt3067	2003 Aug 28.32587	2,452,879.825868	400	22.038
nt3079	2003 Aug 28.35605	2,452,879.856042	400	22.498
nt3080	2003 Aug 28.36082	2,452,879.860810	400	22.513
nt3083	2003 Aug 28.37516	2,452,879.875150	400	22.389
nt3084	2003 Aug 28.37992	2,452,879.879907	400	22.374
nt3093	2003 Aug 28.40996	2,452,879.909942	400	21.864
nt3094	2003 Aug 28.41477	2,452,879.914757	400	21.788
nt3108	2003 Aug 28.44225	2,452,879.942234	400	21.550
nt3109	2003 Aug 28.44701	2,452,879.946991	400	21.471
nt3132	2003 Aug 28.48418	2,452,879.984167	400	21.411
nt3133	2003 Aug 28.49170	2,452,879.991690	400	21.369
nt3164	2003 Aug 28.53695	2,452,880.036933	400	21.405
nt3165	2003 Aug 28.54172	2,452,880.041713	400	21.458
nt3187	2003 Aug 28.57313	2,452,880.073113	400	21.644
nt3188	2003 Aug 28.57790	2,452,880.077882	400	21.659
nt3215	2003 Aug 28.61676	2,452,880.116748	400	22.043
nt3216	2003 Aug 28.62153	2,452,880.121516	400	22.181
nt1.034	2003 Aug 27.27855	2,452,909.778553	300	21.600
nt1.035	2003 Aug 27.28337	2,452,909.783368	300	21.553
nt1.067	2003 Aug 27.42997	2,452,909.929965	300	21.675
nt1.068	2003 Aug 27.43473	2,452,909.934734	300	21.709
nt1.089	2003 Aug 27.53125	2,452,910.031238	300	21.948
nt1.090	2003 Aug 27.53605	2,452,910.036042	300	21.812
nt2.032	2003 Aug 28.27564	2,452,910.775637	300	21.643
nt2.033	2003 Aug 28.28043	2,452,910.780428	300	21.631
nt2.053	2003 Aug 28.37271	2,452,910.872708	300	22.301
nt2.054	2003 Aug 28.37751	2,452,910.877512	300	22.267
nt2.063	2003 Aug 28.42250	2,452,910.922500	300	21.719
nt2.064	2003 Aug 28.42730	2,452,910.927292	300	21.644
nt2.080	2003 Aug 28.49909	2,452,910.999086	300	21.327
nt2.081	2003 Aug 28.50389	2,452,911.003889	300	21.321
nt2.090	2003 Aug 28.55245	2,452,911.052442	300	21.453
nt2.091	2003 Aug 28.55725	2,452,911.057245	300	21.472
nt2.166	2003 Aug 30.34785	2,452,912.847847	400	22.267
nt2.167	2003 Aug 30.35398	2,452,912.853981	400	22.259
nt2.195	2003 Aug 30.48012	2,452,912.980116	400	21.334
nt2.196	2003 Aug 30.48597	2,452,912.985961	400	21.379

[a] Image number.
[b] Decimal Universal Date at the start of the integration.
[c] Julian Date at the start of the integration. No light-time correction has been made in the table.
[d] Exposure time for the image.
[e] Apparent red magnitude; uncertainties are ± 0.03 to ± 0.04.

The absolute magnitude of a solar system object, $m_R(1, 1, 0)$, is the hypothetical magnitude the object would have if it were at heliocentric (R) and geocentric (Δ) distances of 1 AU and had a phase angle (α) of $0°$. We use the relation $m_R(1, 1, 0) = m_R - 5 \log R\Delta - \beta\alpha$ to find the absolute magnitude by correcting for the geometric and phase-angle effects in the 2001 QG_{298} observations. Here m_R is the apparent red magnitude of the object and β is the phase function. Using the nominal value of $\beta = 0.16$ mag deg^{-1} for KBOs at low phase angles (Sheppard & Jewitt 2002, 2004) and data from Table 1, we find that 2001 QG_{298} has $m_R(1, 1, 0) = 6.28 \pm 0.02$ at maximum light and $m_R(1, 1, 0) = 7.42 \pm 0.02$ mag at minimum light. If attributed to a rotational variation of the cross section, this corresponds to a ratio of maximum to minimum areas of 2.85 : 1.

The effective radius of an object can be calculated using the relation $m_R(1, 1, 0) = m_\odot - 2.5 \log [p_R r_e^2/(2.25 \times 10^{16})]$, where $m_\odot$ is the apparent red magnitude of the Sun (-27.1),

TABLE 3
B-Band, *V*-Band, and *R*-Band Observations at Keck

Image[a]	UT Date[b]	Julian Date[c]	Exp.[d] (s)	Mag.
lred0078	2003 Aug 30.37786	2,452,881.877861	150	22.391[e]
lred0084	2003 Aug 30.40107	2,452,881.901076	150	22.070[e]
lred0120	2003 Aug 30.51921	2,452,882.019213	150	21.391[e]
lred0121	2003 Aug 30.52202	2,452,882.022027	150	21.369[e]
lred0082	2003 Aug 30.39546	2,452,881.895460	150	22.803[f]
lred0083	2003 Aug 30.39828	2,452,881.898285	150	22.734[f]
lred0118..................	2003 Aug 30.51329	2,452,882.013295	150	21.981[f]
lred0119..................	2003 Aug 30.51642	2,452,882.016423	150	22.013[f]
lred0079	2003 Aug 30.38170	2,452,881.881700	300	23.917[g]
lred0080	2003 Aug 30.38623	2,452,881.886232	300	23.865[g]
lred0081	2003 Aug 30.39075	2,452,881.890758	300	23.896[g]
lred0114..................	2003 Aug 30.49488	2,452,881.994882	300	22.945[g]
lred0115..................	2003 Aug 30.49949	2,452,881.999492	300	22.980[g]
lred0116..................	2003 Aug 30.50404	2,452,882.004046	300	23.013[g]
lred0117..................	2003 Aug 30.50860	2,452,882.008606	300	23.010[g]

[a] Image number.
[b] Decimal Universal Date at the start of the integration.
[c] Julian Date at the start of the integration. No light-time correction has been made in the table.
[d] Exposure time for the image.
[e] Apparent red magnitude; uncertainties are ± 0.02.
[f] The apparent magnitude is for the *V* band; uncertainties are ± 0.03
[g] The apparent magnitude is for the *B* band; uncertainties are ± 0.04. In the *B* band, only light longward of 0.460 μm was observed, because of the dichroic.

p_R is the red geometric albedo, and r_e (km) is the effective circular radius of the object. If we assume an albedo of 0.04 (0.10), this corresponds to effective circular radii at maximum and minimum light of about 158 (100) km and 94 (59) km, respectively. At the mean absolute magnitude of 6.85 mag, the effective circular radius is 122 (77) km.

4. ANALYSIS

Only three other objects in the solar system larger than 25 km in radius are known to have light-curve ranges greater than 1.0 mag (Table 4). Following Jewitt & Sheppard (2002), we discuss three possible models of rotational variation to try to compare the objects from Table 4 with 2001 QG_{298}.

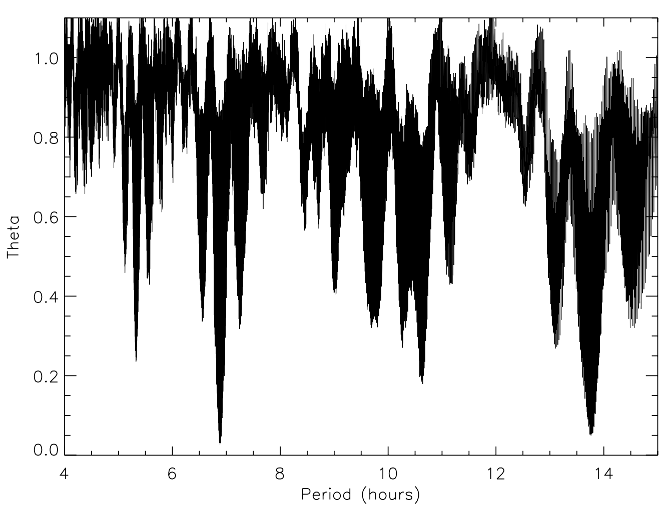

Fig. 1.—Phase dispersion minimization (PDM) plot for 2001 QG_{298}. A smaller Θ corresponds to a better fit. Best fits from this plot are the 6.8872 hr single-peaked fit and the 13.7744 hr double-peaked fit. Both are flanked by alias periods.

4.1. *Albedo Variation*

On asteroids, albedo variations contribute brightness variations that are usually less than about 10% to 20% (Degewij, Tedesco, & Zellner 1979). Rotationally correlated color variations may be seen if the albedo variations are large, since materials with markedly different albedos may differ compositionally. As seen in Table 4, Saturn's satellite Iapetus is the only object in which variations $\geq$1 mag are explained through albedo. The large albedo contrast on Iapetus is likely a special consequence of its synchronous rotation and the anisotropic impact of material trapped in orbit about Saturn onto its leading hemisphere (Cook & Franklin 1970). Iapetus shows clear rotational color variations [$\Delta(B-V) \sim 0.1$ mag] that are correlated with the rotational albedo variations (Millis 1977) and which would be detected in 2001 QG_{298} given the quality of our data. The special circumstance of Iapetus is without obvious analogy in the Kuiper belt, and we do not believe that it is a good model for the extreme light curve of 2001 QG_{298}.

Pluto shows a much smaller variation (about 0.3 mag) thought to be caused by albedo structure (Buie, Tholen, & Wasserman 1997). Pluto is so large that it can sustain an atmosphere, which may contribute to amplifying its light-curve range by allowing surface frosts to condense on brighter (cooler) spots. Thus, brighter spots grow brighter while darker (hotter) spots grow darker through the sublimation of ices. This positive feedback mechanism requires an atmosphere and is unlikely to be relevant on a KBO as small as 2001 QG_{298}.

While we cannot absolutely exclude surface markings as the dominant cause of 2001 QG_{298}'s large rotational brightness variation, we are highly skeptical of this explanation. We measure no color variation with rotation, there appear to be

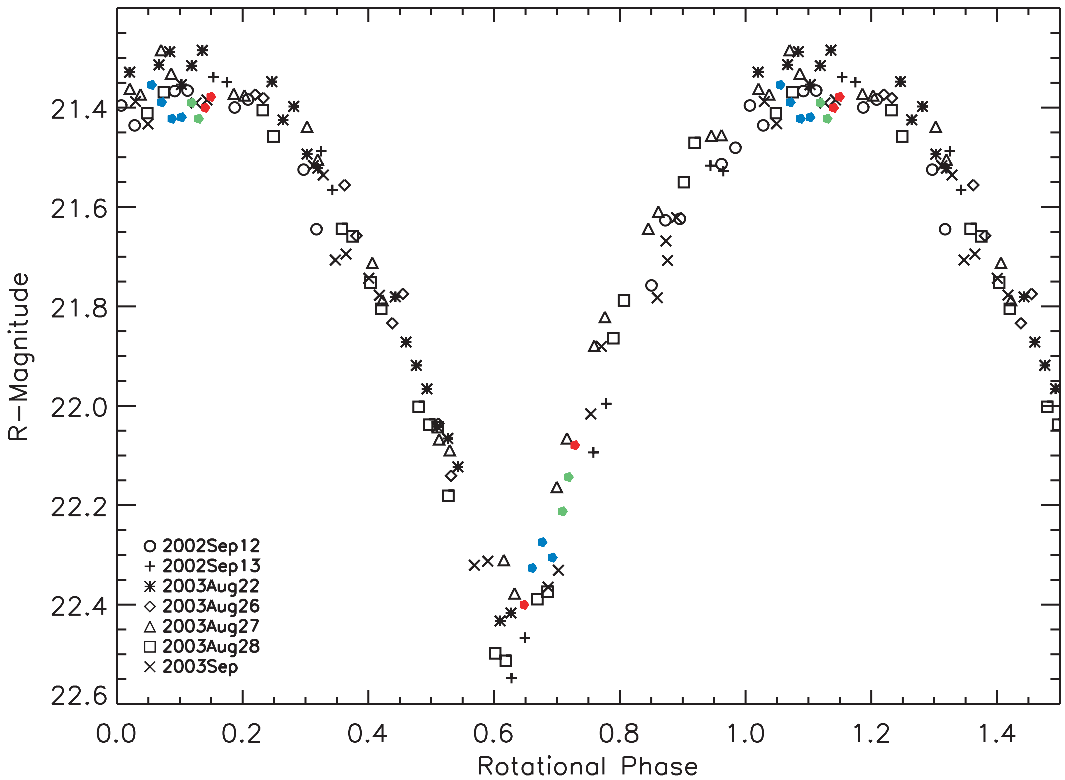

FIG. 2.—Phased data from all the observations in 2002 and 2003 of 2001 QG_{298}. The period has been phased to 6.8872 hr, which is the best-fit single-peaked period. Filled colored symbols are data taken in the B band (*blue*), V band (*green*), and R band (*red*) at the Keck I Telescope on UT August 30. All other symbols are R-band data from the various nights of observations at the UH 2.2 m telescope. The B and V points have been shifted according to their color differences from the R band ($V-R = 0.60$ and $B-V = 1.00$). No color variation is seen between maximum and minimum light. The uncertainty on each photometric observation is ± 0.03 mag.

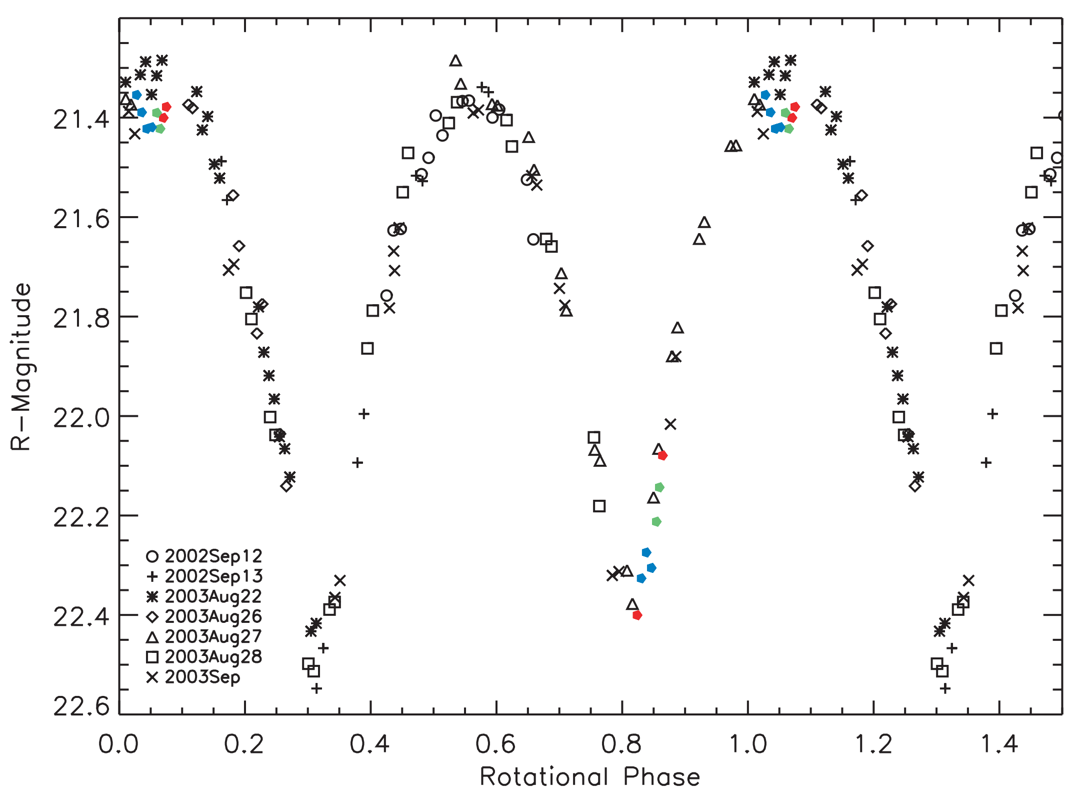

FIG. 3.—Same as Fig. 2, but for a period phased to 13.7744 hr, which is the best-fit double-peaked period. There appear to be two distinct minima. The minima appear to be more "notched" compared with the flatter maxima. No color variation is seen between maximum and minimum light. The uncertainty for each photometric observation is ± 0.03 mag.

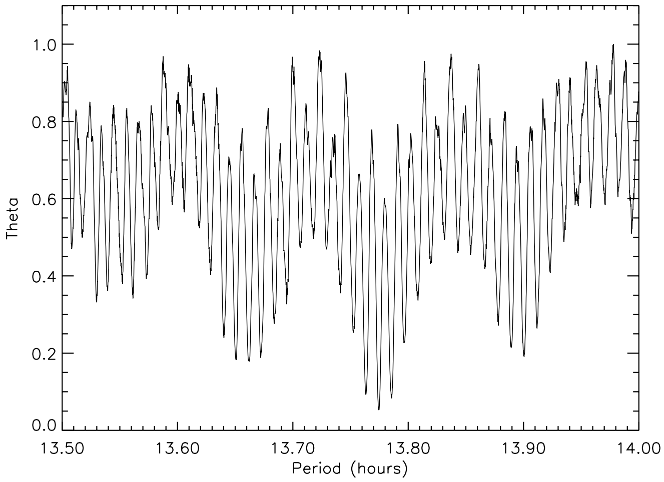

FIG. 4.—Closer view of the PDM plot for 2001 QG_{298} around the double-peaked period at 13.7744 hr. The best fit is flanked by aliases from separation of the three data sets obtained for this object. Only the center PDM peak fits the data once they are phased together.

two distinct minima, and the range is so large as to be beyond reasonable explanation from albedo alone.

4.2. *Aspherical Shape*

Since surface markings are most likely not the cause of the light curve, the observed photometric variations are probably caused by changes in the projected cross section of an elongated body in rotation about its minor axis. The rotation period of an elongated object should be twice the single-peaked light-curve period because of the projection of both long axes (two maxima) and short axes (two minima) during one full rotation. If the body is elongated, we can use the ratio of maximum to minimum brightness to determine the projection of the body shape into the plane of the sky. The rotational brightness range of a triaxial object with semiaxes $a \geq b \geq c$ in rotation about the c-axis and viewed equatorially is

$$\Delta m = 2.5 \log (a/b), \tag{1}$$

where Δm is expressed in magnitudes. This gives a lower limit to a/b because of the effects of projection. Using Δm = 1.14 for 2001 QG_{298}, we find the lower limit is a/b = 2.85. This corresponds to a = 267 and b = 94 km for the geometric albedo 0.04 case and a = 169 and b = 59 km for an albedo of 0.10.

It is possible that 2001 QG_{298} is elongated and able to resist gravitational compression into a spherical shape by virtue of its intrinsic compressive strength. However, observations of asteroids in the main belt suggest that only the smallest ($\sim$0.1 km sized) asteroids are in possession of a tensile strength sufficient to resist rotational deformation (Pravec, Harris, & Michalowski 2003). Observations of both asteroids and planetary satellites suggest that many objects with radii $\geq$50 to 75 km have shapes controlled by self-gravity, not by material strength (Farinella 1987; Farinella & Zappalà 1997). The widely accepted explanation is that these bodies are internally weak because they have been fractured by numerous past impacts. This explanation is also plausible in the Kuiper belt, where models attest to a harsh collisional environment at early times (e.g., Davis & Farinella 1997). We feel that the extraordinarily large amplitude of 2001 QG_{298} is unlikely to be caused by elongation of the object sustained by its own material strength, although we cannot rule out this possibility.

Structurally weak bodies are susceptible to rotational deformation. The 1000 km scale KBO (20000) Varuna (rotation period 6.3442 $\pm$ 0.0002 hr and light-curve range 0.42 $\pm$ 0.02 mag) is the best current example in the Kuiper belt (Jewitt & Sheppard 2002). In the main asteroid belt, 216 Kleopatra has a very short period (5.385 hr) and large light-curve range (1.18 mag, corresponding to axis ratio $\sim$2.95 : 1 and dimensions $\sim$217 $\times$ 94 km; Table 4). Kleopatra has been observed to be a highly elongated body through radar and high-resolution imaging, and the most likely explanation is that 216 Kleopatra is rotationally deformed (Leone et al. 1984; Ostro et al. 2000; Hestroffer et al. 2002; Washabaugh & Scheeres 2002). Is rotational elongation a viable model for 2001 QG_{298}?

The critical rotation period ($T_{\rm crit}$) at which centripetal acceleration equals gravitational acceleration toward the center of a rotating spherical object is

$$T_{\rm crit} = \left(\frac{3\pi}{G\rho}\right)^{1/2}, \tag{2}$$

where G is the gravitational constant and ρ is the density of the object. With ρ = 1000 kg m^{-3}, the critical period is about 3.3 hr. Even at longer periods, real bodies will suffer centripetal deformation into triaxial aspherical shapes that depend on their density, angular momentum, and material strength. The limiting equilibrium shapes of rotating strengthless fluid bodies have been well studied by Chandrasekhar (1987), and a detailed discussion in the context of the KBOs can be found

TABLE 4
LARGE OBJECTS WITH EXTREME LIGHT CURVES

Name	Type	$a \times b$ (km)	Δ m (mag)	Period (hr)	Cause[a]	Ref.
Iapetus	Saturn satellite	715 × 715	2	1903.9	AL	1
624 Hektor	Jupiter Trojan	150 × 75	1.1	6.921	CB	2
216 Kleopatra	Main-belt asteroid	109 × 47	1.18	5.385	JE/CB	3
2001 QG_{298}	Kuiper belt object	267 × 94	1.14	13.7744	CB	4

NOTE.—Objects that have effective radii larger than 25 km and light curves with peak-to-peak amplitudes greater than 1 mag.
[a] The dominant cause or most probable dominant cause for the amplitude of the light curve: (AL) albedo; (CB) contact binary; (JE) Jacobi triaxial rotational ellipsoid.

REFERENCES.—(1) Millis 1977; (2) Dunlap & Gehrels 1969; Hartmann & Cruikshank 1978; Weidenschilling 1980; Leone et al. 1984; Lagerkvist et al. 1989; (3) Scaltriti & Zappalà 1978; Tholen 1980; Leone et al. 1984; Lagerkvist et al. 1989; Ostro et al. 2000; Hestroffer et al. 2002; Washabaugh & Scheeres 2002; (4) this work.

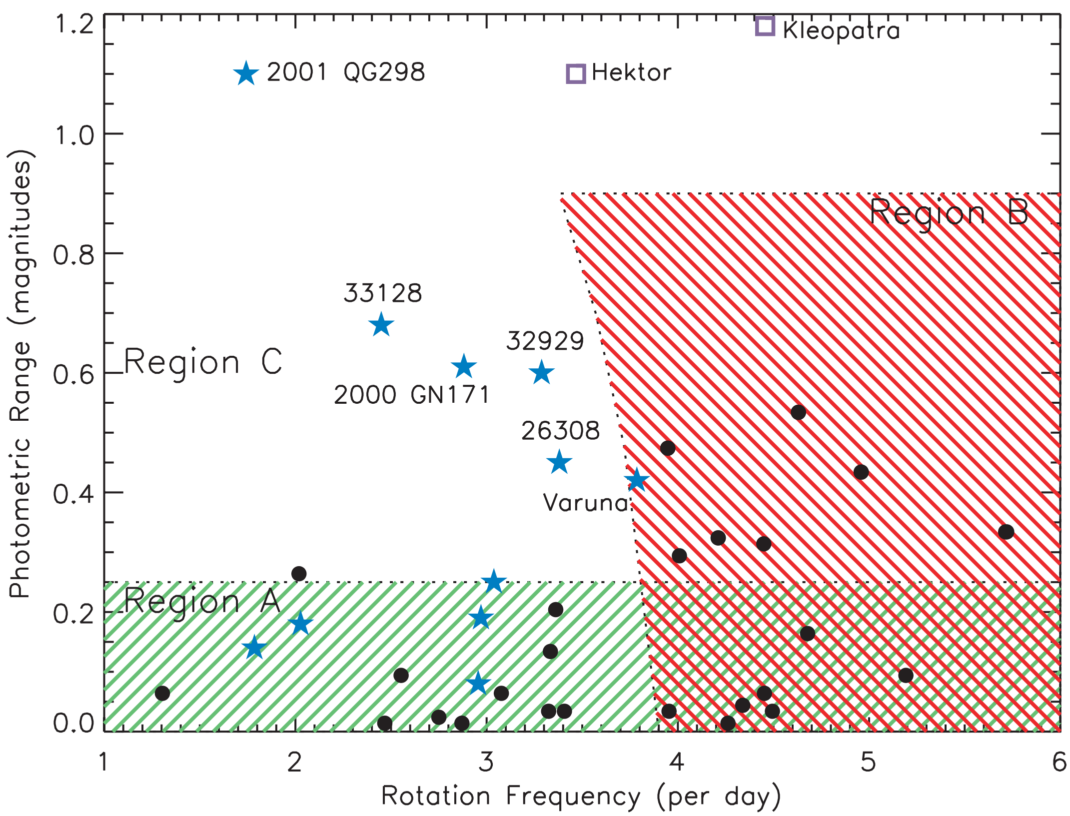

Fig. 5.—Modification of Fig. 4 from Leone et al. (1984). We show the rotation periods and photometric ranges of known KBO light curves and the larger asteroids. The regions are defined as follows: (A) The range of the light curve could be equally well caused by albedo, elongation, or binarity. (B) The light-curve range is most likely caused by rotational elongation. (C) The light-curve range is most likely caused by binarity of the object. Stars denote KBOs, circles denote main-belt asteroids (radii ≥ 100 km), and squares denote the Trojan 624 Hektor and the main-belt asteroid 216 Kleopatra. Objects just to the left of region B would have to have densities significantly less than 1000 kg m^{-3} in order to be elongated from rotational angular momentum. Binary objects are not expected to have photometric ranges above 1.2 mag. The 23 KBOs that have photometric ranges below our photometric uncertainties ($\sim$0.1 mag) in our Hawaii survey have not been plotted, since their periods are unknown. These objects would all fall into region A. The asteroids have been plotted at their expected mean projected viewing angle of 60° in order to more directly compare with the KBOs of unknown projection angle.

in Jewitt & Sheppard (2002). We briefly mention here that triaxial "Jacobi" ellipsoids with large angular momenta are rotationally elongated and generate light curves with substantial ranges when viewed equatorially.

Leone et al. (1984) have analyzed rotational equilibrium configurations of strengthless asteroids in detail (see Fig. 5). They show that the maximum photometric range of a rotational ellipsoid is 0.9 mag: more-elongated objects are unstable to rotational fission. The 1.14 mag photometric range of 2001 QG_{298} exceeds this limit. In addition, the 13.7744 hr (two-peaked) rotation period is much too long to cause significant elongation for any plausible bulk density (Fig. 5). For these reasons, we do not believe that 2001 QG_{298} is a single rotationally distorted object.

4.3. *Binary Configurations*

A third possible explanation for the extreme light curve of 2001 QG_{298} is that this is an eclipsing binary. A wide separation (sum of the orbital semimajor axes much larger than the sum of the component radii) is unlikely because such a system would generate a distinctive "notched" light curve that is unlike the light curve of 2001 QG_{298}. In addition, a wide separation would require unreasonably high bulk density of the components in order to generate the measured rotational period. If 2001 QG_{298} is a binary, then the components must be close or in contact. We next consider the limiting case of a contact binary.

The axis ratio of a contact binary consisting of equal spheres is $a/b = 2$, corresponding to a light-curve range $\Delta m = 0.75$ mag, as seen from the rotational equator. At the average viewing angle $\theta = 60°$, we would expect $\Delta m = 0.45$ mag. The rotational variation of 2001 QG_{298} is too large to be explained as a contact binary consisting of two equal spheres. However, close binary components of low strength should be elongated by mutual tidal forces, giving a larger light-curve range than possible in the case of equal spheres (Leone et al. 1984). The latter authors find that the maximum range for a tidally distorted nearly contact binary is 1.2 mag, compatible with the 1.14 mag range of 2001 QG_{298} (Fig. 5). The contact binary hypothesis is the likely explanation of 624 Hektor's light curve (Hartmann & Cruikshank 1978; Weidenschilling 1980; Leone et al. 1984) and could also explain 216 Kleopatra's light curve (Leone et al. 1984; Ostro et al. 2000; Hestroffer et al. 2002).

We suggest that the relatively long double-peaked period (13.7744 ± 0.0004 hr) and large photometric range (1.14 ± 0.04 mag) of 2001 QG_{298}'s light curve are best understood if the body is a contact binary or near-contact binary viewed from an approximately equatorial perspective. The large range suggests that the components are of similar size and are distorted by their mutual tidal interactions. Using the calculations from Leone et al. (1984), who take into account the mutual deformation of close, strengthless binary components, we find that the density of these objects must be $\sim$1000 kg m^{-3} in

TABLE 5

POSSIBLE CONTACT BINARIES IN THE KUIPER BELT

Name	H^{a} (mag)	$\Delta m_R{}^{b}$ (mag)	Period[c] (hr)	Probability[d]	Ref.
2001 QG_{298}	6.85	1.14 ± 0.04	13.7744 ± 0.0004	Very high	1
2000 GN_{171}	5.98	0.61 ± 0.03	8.329 ± 0.005	High	2
(33128) 1998 BU_{48}	7.2	0.68 ± 0.04	9.8 ± 0.1	High	2
(26308) 1998 SM_{165}	5.8	0.45 ± 0.03	7.1 ± 0.1	Medium	2, 3
(32929) 1995 QY_9	7.5	0.60 ± 0.04	7.3 ± 0.1	Medium	2
(20000) Varuna = 2000 WR_{106}	3.21	0.42 ± 0.03	6.34 ± 0.01	Low	4

[a] Absolute magnitude.
[b] The peak-to-peak range of the light curve.
[c] The light-curve period if there are two maxima per period.
[d] Probability that the object is a contact or nearly contact binary.
REFERENCES.—(1) This work; (2) Sheppard & Jewitt 2002; (3) Romanishin et al. 2001; (4) Jewitt & Sheppard 2002.

order to remain bound in a binary system separated by the Roche radius (which is just over twice the component radius). If we assume that the albedo of both objects is 0.04, the effective radius of each component is about 95 km as found above. Using this information, we find from Kepler's third law that if the components are separated, they would be about 300 km apart. This separation as seen on the sky (0."01) is small enough to have escaped resolution with current technology.

Further, we point out that the maximum of the light curve of 2001 QG_{298} is more nearly U-shaped (or flattened) than is the V-shaped minimum (Fig. 3). This is also true for 624 Hektor (Dunlap & Gehrels 1969) and may be a distinguishing, though not unique, signature of a contact or nearly contact binary (Zappalà 1980; Leone et al. 1984; Cellino et al. 1985). In comparison, (20000) Varuna, which is probably not a contact binary (see below and Jewitt & Sheppard 2002), does not show significant differences in the curvature of the light-curve maxima and minima.

In short, while we cannot prove that 2001 QG_{298} is a contact binary, we find by elimination of other possibilities that this is the most convincing explanation of its light curve.

4.4. *Fraction of Contact Binaries in the Kuiper Belt*

The distribution of measured light-curve properties is shown in Figure 5 (adapted from Fig. 4 of Leone et al. 1984). There, region A corresponds to the low rotational range objects (of any period) in which the variability can be plausibly associated with surface albedo markings. Region B corresponds to the rotationally deformed Jacobi ellipsoids, while region C marks the domain of the close binary objects. Plotted in the figure are the light-curve periods and ranges for KBOs from the HKBVP (Jewitt & Sheppard 2002; Sheppard & Jewitt 2002, 2004). We also show large main-belt asteroids.[2] Once again we note that the measured KBO ranges should, in most cases, be regarded as lower limits to the range because of the possible effects of projection into the plane of the sky.

Of the 34 KBOs in our sample, five fall into region C in Figure 5. Of these, 2001 QG_{298} is by far the best candidate for being a contact or nearly contact binary system, since it alone has a range between the $\Delta m_R \sim 0.9$ mag limit for a single rotational equilibrium ellipsoid and the $\Delta m_R \sim 1.2$ mag limit for a mutually distorted close binary (Table 5). It is also rotating too slowly to be substantially distorted by its own spin (Fig. 5). Both (33128) 1998 BU_{48} and 2000 GN_{171} are good candidates that have large photometric ranges and relatively slow periods. KBOs (26308) 1998 SM_{165} and (32929) 1995 QY_9 could be rotationally deformed ellipsoids, but their relatively slow rotations would require densities much lower than that of water, a prospect that we consider unlikely.

We next ask what might be the abundance of contact or close binaries in the Kuiper belt. As a first estimate, we assume that we have detected one such object (2001 QG_{298}) in a sample of 34 KBOs observed with adequate time resolution. The answer depends on the magnitude of the correction for projection effects caused by the orientation of the rotation vector with respect to the line of sight. This correction is intrinsically uncertain, since it depends on unknowns such as the scattering function of the surface materials of the KBO as well as on the detailed shape. We adopt two crude approximations that should give the projection correction at least to within a factor of a few.

First, we represent the elongated shape of the KBO by a rectangular block with dimensions $a > b = c$. The light-curve range varies with angle from the equator, θ, in this approximation as

$$\Delta m = 2.5 \log \left[\frac{1 + \tan\theta}{(b/a) + \tan\theta} \right]. \quad (3)$$

For the limiting case of a highly distorted contact binary with $\Delta m = 1.2$ mag at $\theta = 0^\circ$, equation (3) gives $a/b = 3$. We next assume that the range must fall between 0.9 and 1.2 mag in order for us to make an assignment of likely binary structure (Fig. 6). As noted above, only 2001 QG_{298} satisfies this condition among the known objects. We find, from equation (3) with $a/b = 3$, that $\Delta m = 0.9$ mag is reached at $\theta = 10^\circ$. The probability that Earth would lie within 10° of the equator of a set of randomly oriented KBOs is $P(\theta \leq 10^\circ) = 0.17$. Therefore, the detection of one KBO with 0.9 mag $\leq \Delta m \leq$ 1.2 mag implies that the fractional abundance of similarly elongated objects is $f \sim 1/(34P) \sim 17\%$.

As a separate check on this estimate, we next represent the object as an ellipsoid, again with axes $a > b = c$. The photometric range when viewed at an angle θ from the rotational equator is given by

$$\Delta m = 2.5 \log \left(\frac{a}{b}\right) - 1.25 \log \left\{ \left[\left(\frac{a}{b}\right)^2 - 1 \right] \sin^2\theta + 1 \right\}. \quad (4)$$

[2] Data from http://cfa-www.harvard.edu/iau/lists/LightcurveDat.html, updated by A. Harris and B. Warner and based on Lagerkvist, Harris, & Zappalà 1989.

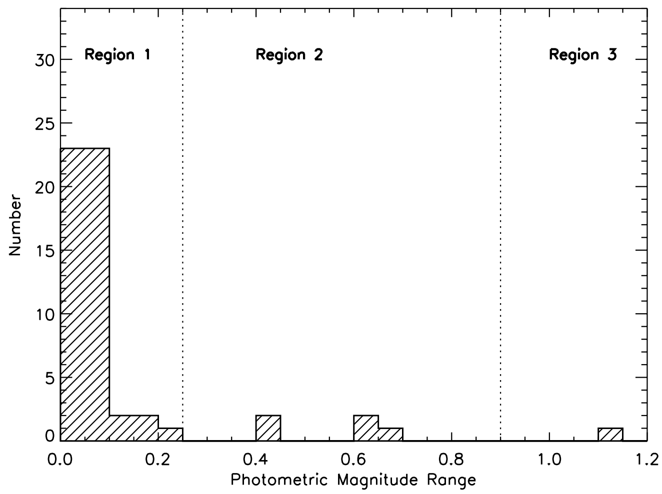

FIG. 6.—Histogram of known KBO photometric ranges. There is a break in known photometric ranges starting around 0.25 mag. The regions are defined as follows: (1) The light-curve range could be dominated by albedo, elongation, or binarity. (2) The light curve is likely dominated by rotational elongation or binarity. (3) The light curve is likely caused by binarity. Data are from our Hawaii Kuiper belt object variability project (Sheppard & Jewitt 2002, 2004).

Substituting $a/b = 3$, the range predicted by equation (4) falls to 0.9 mag at $\theta \sim 17°$. Given a random distribution of the spin vectors, the probability that Earth would lie within 17° of the equator is $P(\theta \leq 17°) = 0.29$. Therefore, the detection of one KBO with a range between 0.9 and 1.2 mag in a sample of 34 objects implies, in this approximation, a fractional abundance of similarly elongated objects near $f \sim 1/(34P) \sim 10\%$.

Given the crudity of the models, the agreement between projection factors from equations (3) and (4) is encouraging. Together, the data and the projection factors suggest that in our sample of 34 KBOs, perhaps three to six objects are as elongated as 2001 QG_{298} but only 2001 QG_{298} is viewed from a sufficiently equatorial perspective that the light curve is distinct. This is consistent with Figure 5, which shows that five of 34 KBOs (15%) from the HKBVP occupy region C of the period-range diagram. Our estimate is very crude and is also a lower limit to the true binary fraction, because close binaries with components of unequal size will not satisfy the 0.9 mag $\leq \Delta m \leq$ 1.2 mag criterion for detection. The key point is that the data are consistent with a substantial close binary fraction in the Kuiper belt.

Figure 5 also shows that there are no large main-belt asteroids (radii $\geq$100 km) in region C, which is where contact binaries with similarly sized components are expected to be. To date, no examples of large binary main-belt asteroids with similar-sized components have been found, even though the main belt has been extensively searched for binarity (see Margot 2002 and references therein). The main-belt asteroids may have had a collisional history significantly different from that of the KBOs.

The contact binary interpretation of the 2001 QG_{298} light curve is clearly nonunique. Indeed, firm proof of the existence of contact binaries will be as difficult to establish in the Kuiper belt as it has been in closer, brighter populations of small bodies. Nevertheless, the data are compatible with a high abundance of such objects. It is interesting to speculate about how such objects could form in abundance. One model of the formation and long-term evolution of wide binaries predicts that such objects could be driven together by dynamical friction or three-body interactions (Goldreich et al. 2002). Objects like 2001 QG_{298} would be naturally produced by such a mechanism.

5. SUMMARY

Kuiper belt object 2001 QG_{298} has the most extreme light curve of any of the 34 objects so far observed in the Hawaii Kuiper Belt Variability Project.

1. The double-peaked light-curve period is 13.7744 $\pm$ 0.0004 hr and the peak-to-peak range is 1.14 $\pm$ 0.04 mag. Only two other minor planets with radii $\geq$25 km (624 Hektor and 216 Kleopatra) and one planetary satellite (Iapetus) are known to show rotational photometric variation greater than 1 mag.
2. The absolute red magnitude is $m_R(1, 1, 0) = 6.28$ at maximum light and 7.42 mag at minimum light. With an assumed geometric albedo of 0.04 (0.10), we derive effective circular radii at maximum and minimum light of 158 (100) and 94 (59) km, respectively.
3. No variation in the *BVR* colors between maximum and minimum light was detected to within photometric uncertainties of a few percent.
4. The large photometric range, differences in the light-curve minima, and long period of 2001 QG_{298} are consistent with and strongly suggest that this object is a contact or near-contact binary, viewed equatorially.
5. If 2001 QG_{298} is a contact binary with similarly sized components, then we conclude that such objects constitute at least 10% to 20% of the Kuiper belt population at large sizes.

We thank John Tonry and Andrew Pickles for help with OPTIC and the remote observing system on the University of Hawaii 2.2 m telescope. We also thank Henry Hsieh for observational assistance, and Jane Luu for comments on the manuscript. This work was supported by a grant to D. J. from the NASA Origins Program.

REFERENCES

Altenhoff, W., Bertoldi, F., & Menten, K. 2004, A&A, 415, 771
Brown, R. H., Cruikshank, D. P., & Pendleton, Y. 1999, ApJ, 519, L101
Buie, M. W., Tholen, D. J., & Wasserman, L. H. 1997, Icarus, 125, 233
Cellino, A., Pannunzio, R., Zappalà, V., Farinella, P., & Paolicchi, P. 1985, A&A, 144, 355
Chandrasekhar, S. 1987, Ellipsoidal Figures of Equilibrium (New York: Dover)
Cook, A. F., & Franklin, F. A. 1970, Icarus, 13, 282
Davis, D. R., & Farinella, P. 1997, Icarus, 125, 50
Degewij, J., Tedesco, E. F., & Zellner, B. 1979, Icarus, 40, 364
Doressoundiram, A., Peixinho, N., de Bergh, C., Fornasier, S., Thébault, P., Barucci, M. A., & Veillet, C. 2002, AJ, 124, 2279 (erratum 125, 1629 [2003])
Duncan, M., Quinn, T., & Tremaine, S. 1988, ApJ, 328, L69
Dunlap, J. L., & Gehrels, T. 1969, AJ, 74, 796
Farinella, P. 1987, in The Evolution of the Small Bodies of the Solar System, ed. M. Fulchignoni & L. Kresák (Amsterdam: North-Holland), 276
Farinella, P., & Zappalà, V. 1997, Adv. Space Res., 19, 181
Fernández, J. A. 1980, MNRAS, 192, 481
Goldreich, P., Lithwick, Y., & Sari, R. 2002, Nature, 420, 643
Hartmann, W. K., & Cruikshank, D. P. 1978, Icarus, 36, 353
Hestroffer, D., Marchis, F., Fusco, T., & Berthier, J. 2002, A&A, 394, 339
Howell, S. B., Everett, M. E., Tonry, J. L., Pickles, A., & Dain, C. 2003, PASP, 115, 1340
Jewitt, D., Aussel, H., & Evans, A. 2001, Nature, 411, 446
Jewitt, D. C., & Luu, J. X. 2001, AJ, 122, 2099
Jewitt, D. C., & Sheppard, S. S. 2002, AJ, 123, 2110

Lacerda, P., & Luu, J. 2003, Icarus, 161, 174
Lagerkvist, C.-I., Harris, A. W., & Zappalà, V. 1989, in Asteroids II, ed. R. P. Binzel, T. Gehrels, & M. S. Matthews (Tucson: Univ. Arizona Press), 1162
Landolt, A. U. 1992, AJ, 104, 340
Lazzarin, M., Barucci, M. A., Boehnhardt, H., Tozzi, G. P., de Bergh, C., & Dotto, E. 2003, AJ, 125, 1554
Leone, G., Farinella, P., Paolicchi, P., & Zappalà, V. 1984, A&A, 140, 265
Luu, J., & Jewitt, D. 1996, AJ, 112, 2310
Margot, J.-L. 2002, Nature, 416, 694
Millis, R. L. 1977, Icarus, 31, 81
Noll, K. S., et al. 2002, AJ, 124, 3424
Oke, J. B., et al. 1995, PASP, 107, 375
Ortiz, J. L., Gutiérrez, P. J., Casanova, V., & Sota, A. 2003, A&A, 407, 1149
Ostro, S. J., et al. 2000, Science, 288, 836
Pravec, P., Harris, A., & Michalowski, T. 2003, in Asteroids III, ed. W. F. Bottke, A. Cellino, P. Paolicchi, & R. P. Binzel (Tucson: Univ. Arizona Press), 113
Romanishin, W., Tegler, S. C., Rettig, T. W., Consolmagno, G., & Botthof, B. 2001, Proc. Natl. Acad. Sci., 98, 11863
Scaltriti, F., & Zappalà, V. 1978, Icarus, 34, 428
Schaefer, B. E., & Rabinowitz, D. L. 2002, Icarus, 160, 52
Sheppard, S. S., & Jewitt, D. C. 2002, AJ, 124, 1757
———. 2004, Earth Moon Planets, in press
Stellingwerf, R. F. 1978, ApJ, 224, 953
Stern, S. A. 2002, AJ, 124, 2300
Tegler, S. C., & Romanishin, W. 2000, Nature, 407, 979
———. 2003, Icarus, 161, 181
Tholen, D. J. 1980, S&T, 60, 203
Tonry, J. L., Burke, B. E., & Schechter, P. L. 1997, PASP, 109, 1154
Trujillo, C. A., & Brown, M. E. 2002, ApJ, 566, L125
Trujillo, C. A., Jewitt, D. C., & Luu, J. X. 2001, AJ, 122, 457
Washabaugh, P. D., & Scheeres, D. J. 2002, Icarus, 159, 314
Weidenschilling, S. J. 1980, Icarus, 44, 807
———. 2002, Icarus, 160, 212
Zappalà, V. 1980, Moon Planets, 23, 345